Available online at www.sciencedirect.com

ScienceDirect

Palaeoworld 29 (2020) 744–751

Palaeoworld

www.elsevier.com/locate/palwor

The Paleogene atmospheric CO_2 concentrations reconstructed using stomatal analysis of fossil *Metasequoia* needles

Yuqing Wang[a], Li Wang[b,c], Arata Momohara[a,*], Qin Leng[d], Yong-Jiang Huang[e]

[a] *Graduate School of Horticulture, Chiba University, 648 Matsudo, Chiba 271-8510, Japan*

[b] *Key Laboratory of Tropical Forest Ecology, Xishuangbanna Tropical Botanical Garden, Chinese Academy of Sciences, Mengla, Yunnan 666303, China*

[c] *Herbarium (HITBC), Xishuangbanna Tropical Botanical Garden, Chinese Academy of Sciences, Mengla, Yunnan 666303, China*

[d] *Department of Science and Technology, College of Arts and Sciences, Bryant University, 1150 Douglas Pike (Suite J), Smithfield, RI 02917, USA*

[e] *Key Laboratory for Plant Diversity and Biogeography of East Asia, Kunming Institute of Botany, Chinese Academy of Sciences, Kunming 650204, China*

Received 24 July 2019; received in revised form 22 December 2019; accepted 4 March 2020

Available online 3 April 2020

Abstract

During the Paleogene, the Earth experienced a global greenhouse climate, which was much warmer and more humid than the present climate. The present global warming is ascribed to increasing levels of atmospheric CO_2 caused by human activity since the industrial revolution; therefore, knowledge of the role of atmospheric CO_2 in the thermal climate during the Paleogene will be helpful for understanding current and future climate. However, unlike for the late Cenozoic, atmospheric CO_2 reconstructions for the Paleogene are still inconsistent and vary between preindustrial-level to values over 4000 ppmv. In this study, we reconstructed the levels of atmospheric CO_2 in the early and middle Paleocene and middle Eocene based on the stomatal index of fossil *Metasequoia* needles collected from four fossil sites in Canada and Japan. We found the atmospheric CO_2 levels during the early and middle Paleocene to be similar to that of the present, and up to twice the present atmospheric CO_2 level was found during the middle Eocene. Our estimated atmospheric CO_2 level supports the hypothesis that the climate changes during the Paleogene cannot be explained merely by atmospheric CO_2 variations, which suggests that atmospheric CO_2 might not have always played a critical role in climate change during these ancient epochs and therefore cannot be a direct analogy for the current global warming.

Keywords: Early–middle Paleocene; Global warming; Middle Eocene; Paleoclimate; Stomatal index

1. Introduction

Atmospheric carbon dioxide (CO_2), as a primary greenhouse gas in the atmosphere, is considered responsible for the current global warming (Houghton et al., 2001; Royer et al., 2004; Fletcher et al., 2008; Stocker et al., 2013). Since atmospheric CO_2 concentration ($[CO_2]$atm) is predicted to increase continuously after reaching levels of 400 ppmv (parts per million by volume) in 2013 (Meinshausen et al., 2011; Masson-Delmotte et al., 2013), a better understanding of a world with high $[CO_2]$atm has become imperative. References for the comparison of greenhouse climates are available from the Paleogene when the Earth experienced a significantly warm and humid condition (Bowen et al., 2004; Hansen et al., 2008; Beerling and Royer, 2011).

The changes in $[CO_2]$atm during the Paleogene have been reconstructed via geochemical modeling (Berner, 1994, 2006; Berner and Kothavala, 2001) and via proxies such as marine carbon (e.g., Pagani et al., 1999, 2005) and boron (e.g., Pearson and Palmer, 2000; Pearson et al., 2009) isotopes and terrestrial proxies such as carbon isotope of palaeosol (e.g., Royer et al., 2001a; Nordt et al., 2002) and liverwort fossils (Fletcher et al., 2008) along with stomata on the fossil leaves of vascular plants. However, $[CO_2]$atm reconstruction based on marine boron isotopes in the Paleogene (Pearson and Palmer, 2000) exhibits significantly higher and more fluctuant values than the data from terrestrial proxies (Sinha and Stott, 1994; Royer et al., 2001b; Royer, 2003). The uncertainty of the reconstructed Paleogene $[CO_2]$atm level makes it difficult to confirm a $[CO_2]$atm-temperature correlation for the late Cenozoic (e.g., Ahn and Brook, 2008; Kürschner et al., 2008; Wang et al., 2015). Some studies support a close correlation between the Paleogene $[CO_2]$atm and temperature (e.g., Bijl

* Corresponding author.
E-mail address: arata@faculty.chiba-u.jp (A. Momohara).

https://doi.org/10.1016/j.palwor.2020.03.002

et al., 2010; Tesfamichael et al., 2017), while some others refute this conclusion based on various hypotheses for climate change besides [CO_2]atm variation (Sloan and Pollard, 1998; Royer et al., 2001b; Ufnar et al., 2004; Shellito et al., 2009). To achieve a better understanding of the effect of [CO_2]atm level on the Paleogene climate change, supplement of the Paleogene [CO_2]atm data based on different proxies becomes necessary.

Among the terrestrial proxies, stomatal [CO_2]atm estimation has been supported by physiological and functional studies (Gray et al., 2000; Kleidon, 2004). Plant taxa, such as *Ginkgo* (Retallack, 2001, 2009; Beerling and Royer, 2002; Royer, 2003; Smith et al., 2010), *Metasequoia* (Royer et al., 2001b; Doria et al., 2011; Maxbauer et al., 2014; Wang et al., 2015), *Gordonia* (Kürschner et al., 2001), and Lauraceae (McElwain, 1998) have been investigated to estimate paleo-[CO_2]atm during the Paleogene. The number of stomata per unit area (stomatal density) and the given number of epidermal cells (stomatal index) on a leaf respond to levels of [CO_2]atm in a species-specific manner (Royer et al., 2001b; Kürschner et al., 2008), which means that taxa existed with limited morphological changes over an extended time period may provide ideal materials for paleo-[CO_2]atm reconstruction over a long geological time.

Along with *Ginkgo* (Retallack, 2001, 2009; Beerling and Royer, 2002; Royer, 2003; Smith et al., 2010), *Metasequoia* Miki *ex* Hu *et* Cheng is a representative plant with evolutionary stasis since the middle Cretaceous. The fossil *Metasequoia* species are generally considered conspecific with the modern species *M. glyptostroboides*, based on morphological and biochemical analyses with its inferred physiology and ecology (LePage et al., 2005). The relationship between the stomatal index (SI) of modern *Metasequoia* leaves and [CO_2]atm has been summarized using associated data under experimentally controlled conditions (Royer et al., 2001b), and the results have been applied to paleo-[CO_2]atm estimation for different ages (Royer et al., 2001b; Doria et al., 2011; Maxbauer et al., 2014; Wang et al., 2015). The extensive and frequent occurrence of *Metasequoia* fossils in time and space (LePage et al., 2005) enables production of detailed [CO_2]atm curve comparable with temperature curve throughout the Paleogene without the noise derived from using different kinds of proxies. However, the Paleogene [CO_2]atm reconstruction based on *Metasequoia* needles (Doria et al., 2011; Maxbauer et al., 2014) is still limited compared with *Ginkgo* leaves. To evaluate the reliability of *Metasequoia* fossils for the Paleogene [CO_2]atm reconstruction, it is necessary to obtain data based on *Metasequoia* needles and compare them with those based on *Ginkgo*.

In this study, we conducted stomatal analysis of fossil *Metasequoia* needles collected from Japan and Canada to estimate [CO_2]atm levels in the early and middle Paleocene and middle Eocene, during which the stomatal-based [CO_2]atm data are still limited. We compared the results with prior published investigations of stomatal and the other proxy-based data, and discussed [CO_2]atm changes during the period to provide fundamental data for understanding current climate change and its trend.

2. Materials and methods

2.1. Fossil locality and geological settings

The well-preserved fossil *Metasequoia* needles used in this study were collected from localities including early Paleocene and middle Eocene strata in northern Japan and middle Paleocene and middle Eocene strata in arctic Canada (Fig. 1). Associated ages, geological settings and other information concerning the collected fossil *Metasequoia* needles can be found in published reports (Tanai, 1979, 1990; Ricketts and Stephenson, 1994; Yang et al., 2005; Hasegawa et al., 2009; Maxbauer et al., 2014; Horiuchi and Uemura, 2017) and are summarized in Table 1. Voucher specimens are housed in the Xishuangbanna Tropical Botanical Garden, Chinese Academy of Sciences.

2.2. Cuticle preparation

The fossil needles were treated with 10–25% hydrochloric acid (HCl) for 2 h, 40% hydrofluoric acid (HF) for 12 h, and 10–25% HCl for at least 1 h to remove the adhering sediments. After the materials were rinsed with distilled water, the middle third of the needles was cut for cuticle preparation. The needle fragments were macerated with a 3–5% sodium hypochlorite (NaClO) solution to remove any remnants of leaf tissue other than the cuticular membrane based on the nature of the leaves. After rinsing with distilled water, the cuticular membranes were stained with 1% safranin O and mounted in glycerol for observation and photographing under the transmitted light microscope (Zeiss Axio Imager A2 with Zeiss AxioCam MRc camera), or directly mounted on aluminum stubs for SEM imagery (Zeiss EVO LS10).

2.3. Stomatal index and the calculation of paleo-[CO_2]atm

Image J (1.43μ, Wayne Rasband, http://rsb.info.nih.gov/ij/) was used to count the number of stomatal complexes (stomatal pore with bounding guard cells) and epidermal cells from photos of cuticular membranes taken with light or electron microscopes (Fig. 2). The field-of-view for stomatal analysis is over 0.03 mm^2 for all images. SI was calculated using Eq. (1) (Salisbury, 1928).

$$SI = \frac{\text{stomatal number}}{\text{epidermal cell number} + \text{stomatal number}} \quad (1)$$

The nonlinear inverse relationship between the SI of *Metasequoia* and [CO_2]atm levels (Eq. (2))was taken from Royer et al. (2001b).

$$[CO_2]atm = \frac{SI - 6.672}{0.003883 \times SI - 0.02897} \quad (2)$$

3. Results

The SI and calculated [CO_2]atm from the prepared cuticular membranes are listed in Table 2 and Table S1. Our data show

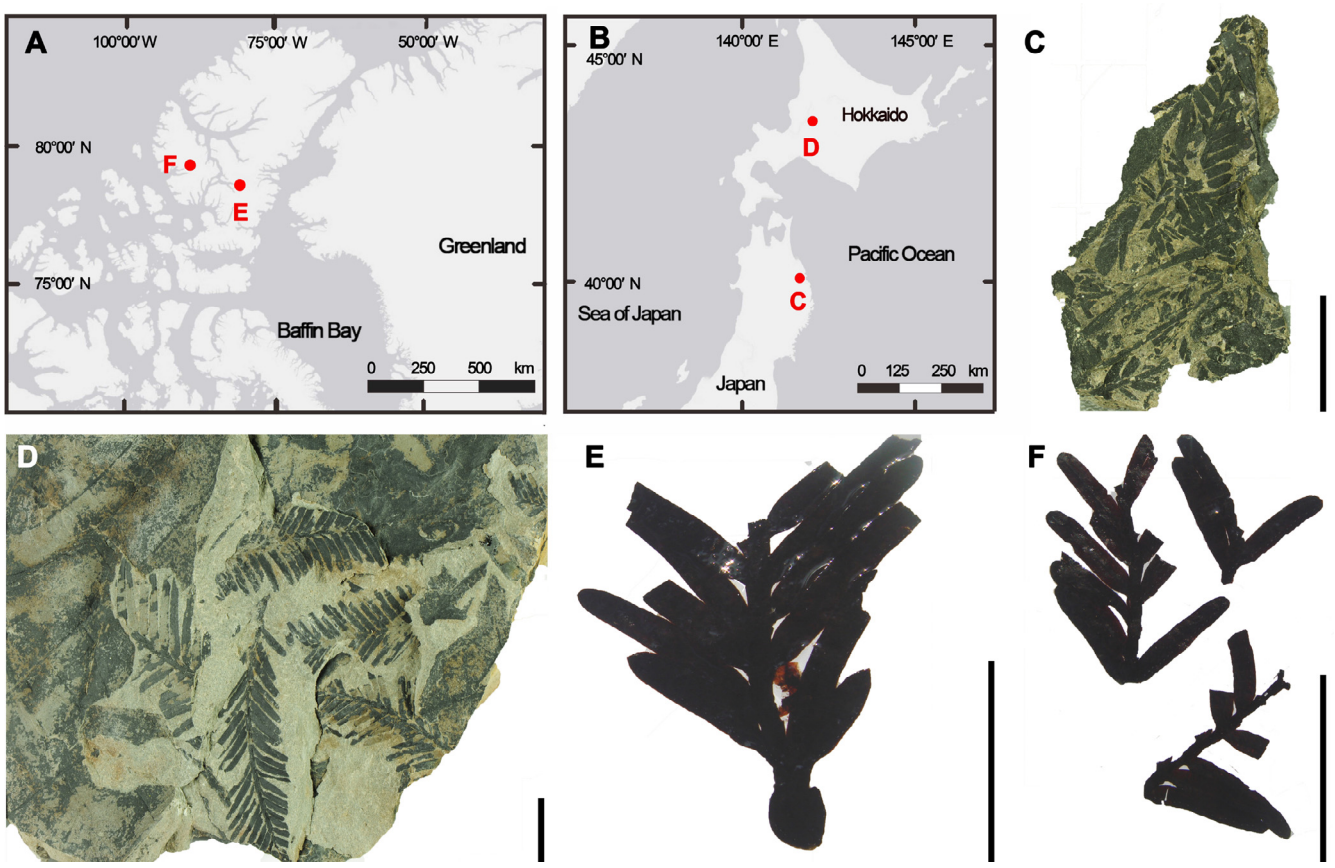

Fig. 1. (A, B) Geological settings of fossil *Metasequoia* needles. (C–F) Fossil *Metasequoia* needles; (C) from Minato Formation, Kuji City, Japan (early Paleocene); (D) from Bibai Formation, Bibai City, Japan (middle Eocene); (E) from Iceberg Bay Formation, Ellesmere Island, Canada (middle Paleocene); (F) from Buchanan Lake Formation, Axel Heiberg Island, Canada (middle Eocene). Scale bar = 1 cm.

Table 1
Information of *Metasequoia* samples used for reconstructing [CO_2]atm level.

Formation	Geologic setting	Epoch (Age)	Dating method	Latitude	Longitude	Reference
Minato	Minato Formation, Noda Group, Kuji City, Iwate Prefecture	early Paleocene (64.3–62.5 Ma)	Fission track dating	40°07′30″N	141°50′15″E	(Horiuchi and Uemura, 2017)
Iceberg Bay	Iceberg Bay Formation, Stenkul Fiord, Ellesmere Island, Canadian Arctic Archipelago	middle Paleocene (ca. 60 Ma)	Stratigraphic study	77°20′58″N	83°26′08″W	(Ricketts and Stephenson, 1994; Yang et al., 2005)
Buchanan Lake	Upper Coal Member of the Buchanan Lake Formation, Axel Heiberg Island, Canadian Arctic Archipelago	middle Eocene (47.9–37.8 Ma)	Stratigraphic study	79°54′55.8″N	89°01′26.8"W	(Maxbauer et al., 2014)
Bibai	Bibai Formation, Ishikari Group, Bibai City, central Hokkaido, Japan	middle Eocene (41–40 Ma)	Fission track dating	43°15′N	141°50′E	(Tanai, 1979, 1990; Hasegawa et al., 2009)

that [CO_2]atm was 308 ± 23 ppmv at ca. 63.4 Ma in the early Paleocene, and 370 ± 27 ppmv at ca. 60 Ma in the middle Paleocene. In the middle Eocene, [CO_2]atm increased to over 473 ± 121 ppmv at 47.9–37.8 Ma, based on materials from the Iceberg Bay Formation. The materials from the Bibai Formation (middle Eocene) show the lowest SI among all *Metasequoia* fossils used in this research, indicating a high [CO_2]atm of 706 ± 321 ppmv at 41–40 Ma.

4. Discussion

4.1. [CO_2]atm level during the Paleocene

Only *Ginkgo* leaves have been used as yet for stomatal index-based [CO_2]atm reconstruction for the Paleocene and the data have provided a continuous record of variations in [CO_2]atm between ca. 54 Ma and ca. 65 Ma (Royer et al.,

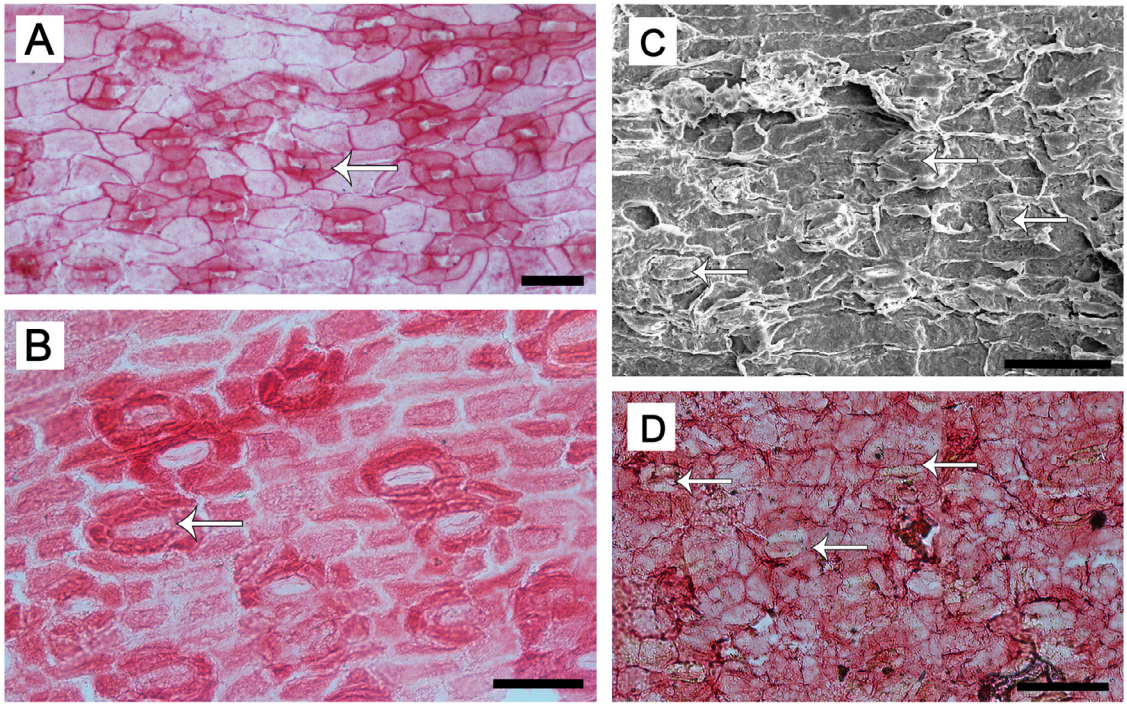

Fig. 2. Microphotographs of lower cuticles of *Metasequoia* needles; (A) from Iceberg Bay Formation, Ellesmere Island, Canada (middle Paleocene); (B) from Minato Formation, Kuji City, Japan (early Paleocene); (C) from Buchanan Lake Formation, Axel Heiberg Island, Canada (middle Eocene); (D) from Bibai Formation, Bibai City, Japan (middle Eocene). The white arrows indicate stomata. (C) was obtained by SEM while all the others were obtained by light microscopy. Scale bar = 50 μm.

Table 2
SI of fossil *Metasequoia* needles and the corresponding $[CO_2]$atm estimates.

Formation	Epoch	Age (Ma)	Number of fossil needles (No.)	SI (%)	$[CO_2]$atm (ppmv)
Minato	early Paleocene	64.3–62.5	10	12.08 ± 1.60	308 ± 23
Iceberg Bay	middle Paleocene	ca. 60	9	9.35 ± 0.41	370 ± 27
Buchanan Lake	middle Eocene	47.9–37.8	12	8.87 ± 1.06	473 ± 121
Bibai	middle Eocene	41–40	9	8.21 ± 0.63	706 ± 321

2001b; Beerling and Royer, 2002; Royer, 2003; Beerling et al., 2009). However, the stomatal $[CO_2]$atm record between 64 Ma and 59 Ma was based only on one datum at 61.5 Ma (Royer, 2003). The fossil *Ginkgo* leaves indicate that $[CO_2]$atm was at 330–470 ppmv during 65–64 Ma, after which it dropped to 317 ppmv at 61 Ma and then increased again to 530–570 ppmv at 59 Ma (Royer, 2003). Subsequently, *Ginkgo*-based $[CO_2]$atm varied mainly between 300 ppmv and 500 ppmv with a peak of 667 ppmv at 55.8 Ma at the Paleocene–Eocene boundary (Royer et al., 2001a; Beerling et al., 2009). The two *Metasequoia*-based $[CO_2]$atm level results in this paper, 308 ppmv at ca. 63 Ma and 370 ppmv at ca. 60 Ma, are the oldest $[CO_2]$atm level data based on the stomatal analysis of *Metasequoia* needles to date. Our data, with narrow error ranges, complete the sequence of *Ginkgo*-based $[CO_2]$atm records with the drop in $[CO_2]$atm values at 63 Ma; and also support the increasing trends in $[CO_2]$atm found between 61 Ma and 58.5 Ma, as demonstrated in the *Ginkgo*-based $[CO_2]$atm records (Royer, 2003) (Fig. 3).

Proxies other than stomatal parameters for $[CO_2]$atm reconstruction during the Paleocene have been derived from alternative terrestrial proxies including the carbon isotopes of paleosols or liverworts, and marine proxies such as the boron isotopes from marine calcium carbonate or carbon isotopes from phytoplankton (Fig. 3). Paleosol-based $[CO_2]$atm was estimated as ca. 400 ppmv in the earliest Paleocene (Nordt et al., 2002) and 100–800 ppmv in the late Paleocene and early Eocene, which exhibits wide variations as compared to other proxies (Sinha and Stott, 1994; Royer et al., 2001b). In addition, the isotope analysis of liverworts indicated a $[CO_2]$atm of 583 ppmv at ca. 58.4 Ma, which is consistent with the *Ginkgo*-based data. However, $[CO_2]$atm reconstruction based on marine boron isotopes in the late Paleocene and the early Eocene (Pearson and Palmer, 2000) exhibits significantly higher values (> 2000 ppmv) than the data from terrestrial proxies (Sinha and Stott, 1994; Royer et al., 2001b; Royer, 2003), along with considerable fluctuations. This boron isotope method, however, is based on the assumption that the boron

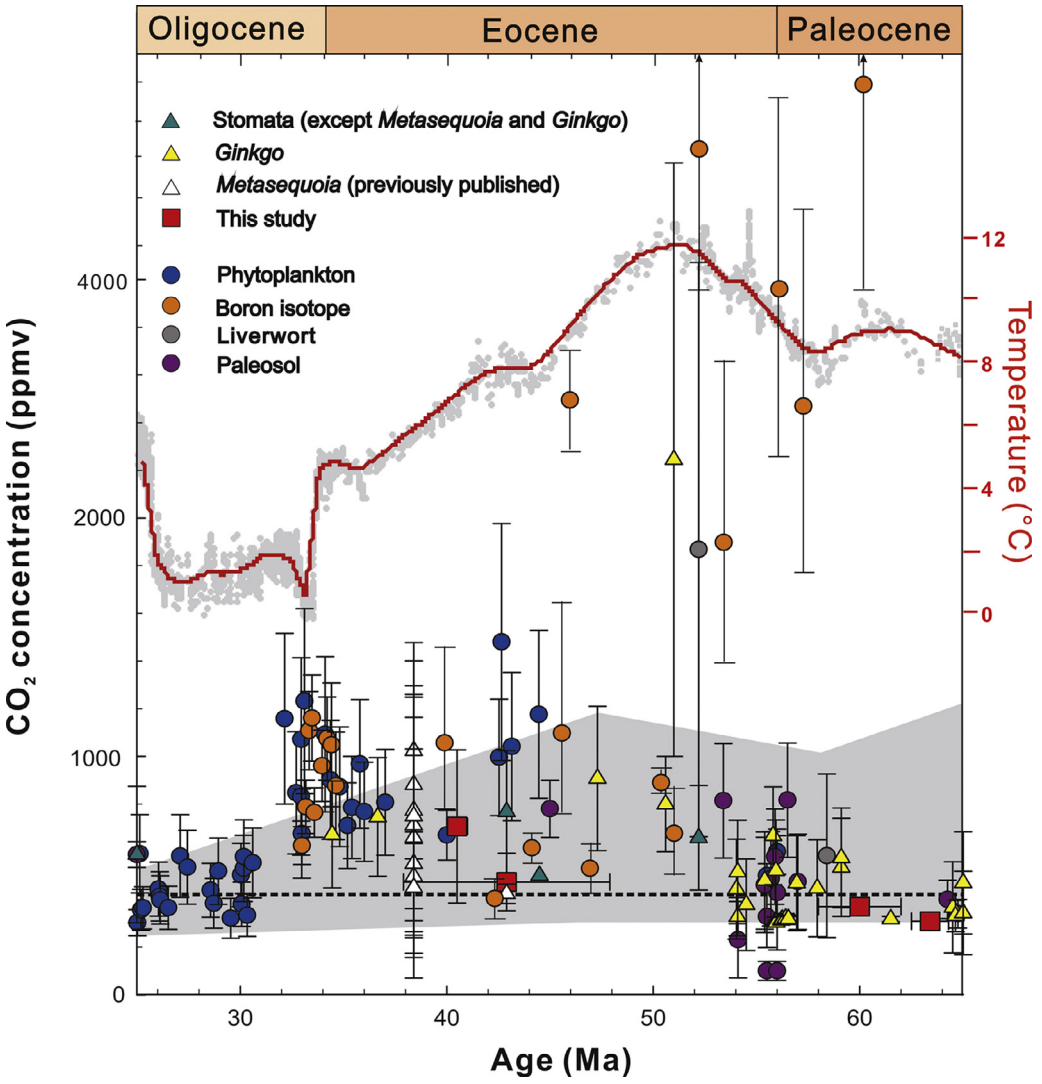

Fig. 3. Atmospheric CO_2 history in the Paleogene, reconstructed by GEOCARB III (gray shade) (Berner and Kothavala, 2001) and different proxies. Including previously published stomatal analyses of *Metasequoia* (Doria et al., 2011; Maxbauer et al., 2014), *Ginkgo* (Retallack, 2001, 2009; Beerling and Royer, 2002; Royer, 2003; Beerling et al., 2009; Smith et al., 2010), and other species (McElwain, 1998; Kürschner et al., 2001; Greenwood et al., 2003), liverworts (Fletcher et al., 2008), and analysis of paleosols (Koch et al., 1992; Sinha and Stott, 1994; Ekart et al., 1999; Royer et al., 2001a; Nordt et al., 2002), phytoplankton (Freeman and Hayes, 1992; Stott, 1992; Pagani, 1999; Pagani et al., 1999, 2005), and boron isotopes (Pearson and Palmer, 2000; Pearson et al., 2009). Deep-sea temperatures (Zachos et al., 2001) are shown in the upper panel. The error bars represent the reported uncertainties. The horizontal dash line indicates the present-day atmospheric CO_2 level (400 ppmv).

isotopic composition of the ocean remains at nearly constant levels throughout time, without changes due to biological processes or differences in temperature, which has not been proved for the Paleocene (Royer et al., 2001a).

Contrary to the current view that global warming is associated with the [CO_2]atm levels, the paleotemperature during the Paleocene was much higher than what it is today, according to marine isotope data (Zachos et al., 2001). The early and middle Paleocene fossil floras also indicate a higher temperature than that of today at mid and high latitudes, according to their physiognomic characters and the fact that the Nearest Living Relatives of these species are also distributed in areas with warmer temperatures (Spicer and Parrish, 1990). The appearance of crocodilians during the Paleocene (Markwick, 1998) in the United States is further proof of a warm environment. Considering the evidence for a warm climate during the early and middle Paleocene, if our stomatal [CO_2]atm reconstruction is correct, factors besides [CO_2]atm are necessary to explain the global warmth during this period. The lower Paleocene [CO_2]atm of this study indicates that the warm climate in the early and middle Paleocene is not comparable to the present global warming because the effect from [CO_2]atm on the increasing global temperature was less apparent than it is in the present. Although the Paleocene–Eocene Thermal Maximum (PETM) has been confirmed to be associated with the release of methane (Dickens et al., 1997; Higgins and Schrag, 2006; Pancost et al., 2007; Winguth et al., 2010), our [CO_2]atm data is from an earlier period. Thus, instead of methane, factors like paleogeography, enhanced meridional heat transport, and high latitude vegetation feedbacks may help to explain this warm period (Royer et al., 2001b).

4.2. Higher [CO_2]atm level than that of today during the middle Eocene

The Earth during the middle Eocene also experienced a long-term period of global warmth, with higher temperatures than those of today, and a decreasing trend in temperature after the early Eocene climatic optimum (Hansen et al., 2008; Bohaty et al., 2009; Wolfe et al., 2017). The stomatal data from this period generally exhibit [CO_2]atm values higher than the present level [CO_2]atm (ca. 400 ppmv), although the data are limited compared with that from the Paleocene. High levels of [CO_2]atm were represented in *Ginkgo* fossils, which indicated [CO_2]atm levels of 907 ppmv at ca. 47.3 Ma (Retallack, 2009). Stomatal analyses of fossil *Gordonia* (Kürschner et al., 2001) and Lauraceous (McElwain, 1998) leaves present a [CO_2]atm level of 500–800 ppmv during 44.5–42.9 Ma. Our [CO_2]atm level data (473 ± 121 ppmv) at 47.9–37.8 Ma in the middle Eocene is lower than that found in these published studies. At the same fossil locality in Axel Heiberg Island, fossil *Metasequoia* needles have previously been used in [CO_2]atm estimations by stomatal analysis (471 ppmv) and carbon isotope analysis based on the plant gas-exchange model (441 ppmv) (Maxbauer et al., 2014). The consistency between their results and ours indicates that fossil *Metasequoia* leaves are reliable for use in [CO_2]atm estimation, and the [CO_2]atm levels presented by this taxon do not vary among researchers or with different methods.

Other stomatal data from the middle Eocene found in this study estimated [CO_2]atm levels of 706 ± 321 ppmv at 41–40 Ma, which is higher than the [CO_2]atm estimation of 47.9–37.8 Ma. However, this value is within the range of values estimated by the stomatal analysis of *Metasequoia* needles from ten fossil-bearing layers in a fossil locality in northwestern Canada, which indicated a series of [CO_2]atm data from ca. 1000 ppmv to ca. 400 ppmv at 38.4 Ma, with a decreasing trend.

Compared with the Paleocene [CO_2]atm data, middle Eocene [CO_2]atm estimated both by stomatal and the other proxies vary over a short time-span. The boron isotope data documented changes in [CO_2]atm from ca. 400 ppmv at ca. 43 Ma to over 1000 ppmv at 39 Ma (Pearson and Palmer, 2000), although boron-based [CO_2]atm data from the middle Eocene generally give lower values than those found in the early Eocene, which vary between 400 ppmv and 2500 ppmv (Pearson and Palmer, 2000). Meanwhile, the [CO_2]atm based on the isotope analysis of phytoplankton also indicated a fluctuation in [CO_2]atm values between ca. 1200 and ca. 650 ppmv during the period from 44 Ma to 40 Ma, although the precision of this method decreases when [CO_2]atm rises to above 750 ppmv (Kump and Arthur, 1999; Royer et al., 2001a).

Different proxies indicate higher [CO_2]atm levels during the middle Eocene, but the relationship between [CO_2]atm and global warming in this age has not been clarified due to the inconsistent results of [CO_2]atm. Plant fossils have recorded a warm climate during the Eocene as well, for example, the northern limit for the distribution of a frost intolerant palm was 20° latitude further north than it is currently in North America (Greenwood and Wing, 1995). Multiple climate proxies also demonstrate an Arctic environment with winter temperatures at or just above freezing point and summer temperatures of ≥ 20°C during the early–middle Eocene (Eberle and Greenwood, 2012). During this warm period, a decrease in temperature since the middle Eocene was detected in marine oxygen isotopes (Zachos et al., 2001), which cannot be explained by the [CO_2]atm variation based on stomatal or other proxy data. Thus, other factors, such as complex feedbacks initiated by tectonic alterations to the ocean basins (Shellito et al., 2009), increased polar stratospheric clouds (Sloan and Pollard, 1998), and increased latent heat transport (Ufnar et al., 2004) may be the complementary warming mechanisms besides [CO_2]atm level increase. However, our understanding of the climate change mechanisms during this greenhouse period is still far from clear.

4.3. Advantages of fossil Metasequoia needles in [CO_2]atm estimation

Metasequoia fossils have been reported in more than 500 localities in the Northern Hemisphere, belonging to various ages from the Cretaceous to the Pleistocene (LePage et al., 2005). This very wide and frequent occurrence of *Metasequoia* fossils in time and space allows the production of an evolutionary curve in [CO_2]atm throughout the whole Cenozoic from use of these fossil needles alone, without the noise derived from using different kinds of proxies. Although several *Metasequoia*-based [CO_2]atm records from the Cenozoic have been published to date (Royer et al., 2001b; Doria et al., 2011; Maxbauer et al., 2014; Wang et al., 2015), the *Metasequoia*-based [CO_2]atm data from the Paleogene are still insufficient compared with data from *Ginkgo*. This may be ascribed to its fragile cuticle as compared to *Ginkgo*. However, the development of fluorescence microscopes, laser scan microscopes and electron scanning microscopes enables much easier observation of such delicate cuticles.

This research demonstrated that the mechanisms that caused the Paleogene climate change were significantly complex, and that variations in [CO_2]atm played a less important role than in today. Thus, studies concerning climate changes during the Neogene and Quaternary will be more helpful for a better understanding of the mechanisms leading to present global warming. Fossil *Metasequoia* needles from the late Cenozoic are very abundant, especially in Japan, and other materials with continuous and high-resolution stratigraphic settings are available for investigation (LePage et al., 2005). Leaf margin analysis and stomatal analysis of a Japanese fossil assemblage has implied a coupled relationship between [CO_2]atm and temperature during the Quaternary (Wang et al., 2018b). Compared with the species that were distributed over a wide range of altitudes, such as *Fagus, Quercus* and *Ginkgo, Metasequoia* is generally limited to floodplains at low altitudes, which can avoid errors in [CO_2]atm estimation caused by the transportation of leaves from higher altitudes before fossilization (Wang et al., 2018a). Since the stomatal index can record rapid [CO_2]atm changes occurring within 100 years (Royer, 2001), *Metasequoia* fossil needles have the potential to provide more detailed information in [CO_2]atm evolutionary history during the Cenozoic.

4. Conclusions

In this study, based on the fossil *Metasequoia* needles, we reconstructed [CO_2]atm for four time intervals during the early and middle Paleocene and middle Eocene. In the early and middle Paleocene (ca. 63−60 Ma), [CO_2]atm was estimated at 300−400, which is a little lower than the present level. During the middle Eocene, [CO_2]atm was estimated at 473 ppmv in 47.9−37.8 Ma and 706 ppmv in 41−40 Ma. The [CO_2]atm values estimated by stomatal index from fossil *Metasequoia* leaves are consistent with those based on *Ginkgo*, which demonstrates the excellence of *Metasequoia* for use as a proxy to demonstrate paleo-[CO_2]atm levels, along with its common and frequent occurrence through the whole Cenozoic. During the Paleogene, climate change under the thermal environment cannot merely be explained by variations in [CO_2]atm; other factors, such as paleogeography, high latitude vegetation feedbacks, increased polar stratospheric clouds, and increased latent heat transport, may be the complementary warming mechanisms. This means that [CO_2]atm played a less crucial role in these ancient epochs.

Acknowledgments

This research was supported by the National Natural Science Foundation of China (No. 31300188), XTBG Postdoctoral Research Funding (No. 119103KP07), State Key Laboratory of Paleobiology and Stratigraphy (Nanjing Institute of Geology and Paleontology, CAS) Open Funding (No. 123108) and the scientific fund from Chiba University. We would like to thank Dr. Zhe-Kun Zhou for advice on lab work and manuscript writing, Drs. Cheng Quan, Hong Yang, Jun-Wu Shu, and Sergei Vikulin for their provision of fossil materials, Dr. Tao Su for help in data analysis, and Dr. Kazuhiko Uemura for the information of the Paleocene fossil locality in Kuji City. We are indebted to the Central Laboratory of Xishuangbanna Tropical Botanical Garden, CAS for providing cuticle observing equipment (light microscope and SEM). We are grateful to two anonymous reviewers for their constructive suggestions and thorough comments on the manuscript.

Supplementary materials

Supplementary material associated with this article can be found in the online version at doi:10.1016/j.palwor.2020.03.002.

References

Ahn, J., Brook, E.J., 2008. Atmospheric CO_2 and climate on millennial time scales during the last glacial period. Science 322, 83–85.

Beerling, D., Royer, D., 2002. Reading a CO_2 signal from fossil stomata. New Phytologist 153, 387–397.

Beerling, D.J., Royer, D.L., 2011. Convergent Cenozoic CO_2 history. Nature Geoscience 4, 418–420.

Beerling, D.J., Fox, A., Anderson, C.W., 2009. Quantitative uncertainty analyses of ancient atmospheric CO_2 estimates from fossil leaves. American Journal of Science 309, 775–787.

Bijl, P.K., Houben, A.J.P., Schouten, S., Bohaty, S.M., Sluijs, A., Reichart, G.-J., Sinninghe Damsté, J.S., Brinkhuis, H., 2010. Transient Middle Eocene atmospheric CO_2 and temperature variations. Science 330, 819–821.

Berner, R.A., 1994. GEOCARB II: A revised model of atmospheric CO_2 over Phanerozoic time. American Journal of Science 301, 182–204.

Berner, R.A., 2006. GEOCARBSULF: A combined model for Phanerozoic atmospheric O_2 and CO_2. Geochimica et Cosmochimica Acta 70, 5653–5664.

Berner, R.A., Kothavala, Z., 2001. GEOCARB III: a revised model of atmospheric CO_2 over Phanerozoic time. American Journal of Science 301, 182–204.

Bohaty, S.M., Zachos, J.C., Florindo, F., Delaney, M.L., 2009. Coupled greenhouse warming and deep-sea acidification in the middle Eocene. Paleoceanography 24, PA2207.

Bowen, G.J., Beerling, D.J., Koch, P.L., Zachos, J.C., Quattlebaum, T., 2004. A humid climate state during the Palaeocene/Eocene thermal maximum. Nature 432, 495.

Dickens, G.R., Castillo, M.M., Walker, J.C., 1997. A blast of gas in the latest Paleocene: Simulating first-order effects of massive dissociation of oceanic methane hydrate. Geology 25, 259–262.

Doria, G., Royer, D.L., Wolfe, A.P., Fox, A., Westgate, J.A., Beerling, D.J., 2011. Declining atmospheric CO_2 during the late Middle Eocene climate transition. American Journal of Science 311, 63–75.

Eberle, J.J., Greenwood, D.R., 2012. Life at the top of the greenhouse Eocene world — A review of the Eocene flora and vertebrate fauna from Canada's High Arctic. Geological Society of America Bulletin 124, 3–23.

Ekart, D.D., Cerling, T.E., Montanez, I.P., Tabor, N.J., 1999. A 400 million year carbon isotope record of pedogenic carbonate: implications for paleoatmospheric carbon dioxide. American Journal of Science 299, 805–827.

Fletcher, B.J., Brentnall, S.J., Anderson, C.W., Berner, R.A., Beerling, D.J., 2008. Atmospheric carbon dioxide linked with Mesozoic and early Cenozoic climate change. Nature Geoscience 1, 43.

Freeman, K.H., Hayes, J., 1992. Fractionation of carbon isotopes by phytoplankton and estimates of ancient CO_2 levels. Global Biogeochemical Cycles 6, 185–198.

Gray, J.E., Holroyd, G.H., Van Der Lee, F.M., Bahrami, A.R., Sijmons, P.C., Woodward, F.I., Schuch, W., Hetherington, A.M., 2000. The HIC signalling pathway links CO_2 perception to stomatal development. Nature 408, 713.

Greenwood, D.R., Wing, S.L., 1995. Eocene continental climates and latitudinal temperature gradients. Geology 23, 1044–1048.

Greenwood, D.R., Scarr, M.J., Christophel, D.C., 2003. Leaf stomatal frequency in the Australian tropical rainforest tree Neolitsea dealbata (Lauraceae) as a proxy measure of atmospheric pCO_2. Palaeogeography, Palaeoclimatology, Palaeoecology 196, 375–393.

Hansen, J., Sato, M., Kharecha, P., Beerling, D., Berner, R., Masson-Delmotte, V., Pagani, M., Raymo, M., Royer, D.L., Zachos, J.C., 2008. Target atmospheric CO_2: Where should humanity aim? Open Atmospheric Science Journal 2, 217–231.

Hasegawa, H., Suzuki, N., Saito, H., 2009. Coal-bearing succession of the middle Eocene Ishikari Group in Sanbi Coal Mine, central Hokkaido. The Journal of the Geological Society of Japan 115, 15–16.

Higgins, J.A., Schrag, D.P., 2006. Beyond methane: towards a theory for the Paleocene−Eocene thermal maximum. Earth and Planetary Science Letters 245, 523–537.

Horiuchi, J., Uemura, K., 2017. Paleocene occurrence of *Pseudotorellia* Florin (Ginkgoales) from Northeast Japan and the Meso−Cenozoic history of *Pseudotorellia* and *Torellia*. Review of Palaeobotany and Palynology 246, 146–160.

Houghton, J., Ding, Y., Griggs, D., Noguer, M., van der Linden, P., Dai, X., Maskell, K., Johnson, C., 2001. IPCC Climate Change: the Scientific Basis. Cambridge University Press, Cambridge, 881 pp.

Kleidon, A., 2004. Optimized stomatal conductance of vegetated land surfaces and its effects on simulated productivity and climate. Geophysical Research Letters 31, L21203.

Koch, P.L., Zachos, J.C., Gingerich, P.D., 1992. Correlation between isotope records in marine and continental carbon reservoirs near the Palaeocene/Eocene boundary. Nature 358, 319–322.

Kump, L.R., Arthur, M.A., 1999. Interpreting carbon-isotope excursions: carbonates and organic matter. Chemical Geology 161, 181–198.

Kürschner, W., Wagner, F., Dilcher, D.L., Visscher, H., 2001. Using fossil leaves for the reconstruction of Cenozoic paleoatmospheric CO_2 concentrations. Geological Perspectives of Global Climate Change 47, 169–189.

Kürschner, W.M., Kvacek, Z., Dilcher, D.L., 2008. The impact of Miocene atmospheric carbon dioxide fluctuations on climate and the evolution of terrestrial ecosystems. Proceedings of the National Academy of Sciences of the United States of America 105, 449–453.

LePage, B.A., Williams, C.J., Yang, H., 2005. The Geobiology and Ecology of *Metasequoia*. Springer, Dordrecht, 434 pp.

Markwick, P.J., 1998. Fossil crocodilians as indicators of Late Cretaceous and Cenozoic climates: implications for using palaeontological data in reconstructing palaeoclimate. Palaeogeography, Palaeoclimatology, Palaeoecology 137, 205–271.

Masson-Delmotte, V., Schulz, M., Abe-Ouchi, A., Beer, J., Ganopolski, A., González Rouco, J., Jansen, E., Lambeck, K., Luterbacher, J., Naish, T., 2013. Information from paleoclimate archives. In: Stocker, T.F., Qin, D., Plattner, G.K., Tignor, M., Allen, S.K., Boschung, J. (Eds.), Climate Change 2013: The Physical Science Basis. Contribution of Working Group I to the Fifth Assessment Report of the Intergovernmental Panel On Climate Change. Cambridge University Press, Cambridge, New York, pp. 383–464.

Maxbauer, D.P., Royer, D.L., LePage, B.A., 2014. High Arctic forests during the middle Eocene supported by moderate levels of atmospheric CO_2. Geology 42, 1027–1030.

McElwain, J.C., 1998. Do fossil plants signal palaeoatmospheric carbon dioxide concentration in the geological past? Philosophical Transactions of the Royal Society B: Biological Sciences 353, 83–96.

Meinshausen, M., Smith, S.J., Calvin, K., Daniel, J.S., Kainuma, M.L.T., Lamarque, J.-F., Matsumoto, K., Montzka, S.A., Raper, S.C.B., Riahi, K., Thomson, A., Velders, G.J.M., van Vuuren, D.P.P., 2011. The RCP greenhouse gas concentrations and their extensions from 1765 to 2300. Climatic Change 109, 213.

Nordt, L., Atchley, S., Dworkin, S., 2002. Paleosol barometer indicates extreme fluctuations in atmospheric CO_2 across the Cretaceous–Tertiary boundary. Geology 30, 703–706.

Pagani, M., 1999. Late Miocene atmospheric CO_2 concentrations and the expansion of C4 grasses. Science 285, 876–879.

Pagani, M., Arthur, M.A., Freeman, K.H., 1999. Miocene evolution of atmospheric carbon dioxide. Paleoceanography 14, 273–292.

Pagani, M., Zachos, J.C., Freeman, K.H., Tipple, B., Bohaty, S., 2005. Marked decline in atmospheric carbon dioxide concentrations during the Paleogene. Science 309, 600–603.

Pancost, R.D., Steart, D.S., Handley, L., Collinson, M.E., Hooker, J.J., Scott, A.C., Grassineau, N.V., Glasspool, I.J., 2007. Increased terrestrial methane cycling at the Palaeocene–Eocene thermal maximum. Nature 449, 332–335.

Pearson, P.N., Palmer, M.R., 2000. Atmospheric carbon dioxide concentrations over the past 60 million years. Nature 406, 695–699.

Pearson, P.N., Foster, G.L., Wade, B.S., 2009. Atmospheric carbon dioxide through the Eocene–Oligocene climate transition. Nature 461, 1110.

Retallack, G.J., 2001. A 300-million-year record of atmospheric carbon dioxide from fossil plant cuticles. Nature 411, 287.

Retallack, G.J., 2009. Greenhouse crises of the past 300 million years. Geological Society of America Bulletin 121, 1441–1455.

Ricketts, B.D., Stephenson, R.A., 1994. The demise of Sverdrup Basin; Late Cretaceous–Paleogene sequence stratigraphy and forward modeling. Journal of Sedimentary Research 64, 516–530.

Royer, D.L., 2001. Stomatal density and stomatal index as indicators of paleoatmospheric CO_2 concentration. Review of Palaeobotany and Palynology 114, 1–28.

Royer, D.L., 2003. Estimating latest Cretaceous and Tertiary atmospheric CO_2 from stomatal indices. Special Papers – Geological Society of America 369, 79–93.

Royer, D.L., Berner, R.A., Beerling, D.J., 2001a. Phanerozoic atmospheric CO_2 change: evaluating geochemical and paleobiological approaches. Earth-Science Reviews 54, 349–392.

Royer, D.L., Wing, S.L., Beerling, D.J., Jolley, D.W., Koch, P.L., Hickey, L.J., Berner, R.A., 2001b. Paleobotanical evidence for near present-day levels of atmospheric CO_2 during part of the Tertiary. Science 292, 2310–2313.

Royer, D.L., Berner, R.A., Montañez, I.P., Tabor, N.J., Beerling, D.J., 2004. CO_2 as a primary driver of Phanerozoic climate. GSA Today 14, 4–10.

Salisbury, E.J., 1928. On the causes and ecological significance of stomatal frequency, with special reference to the Woodland Flora. Philosophical Transactions of the Royal Society B: Biological Sciences 216, 1–65.

Shellito, C.J., Lamarque, J.F., Sloan, L.C., 2009. Early Eocene Arctic climate sensitivity to pCO_2 and basin geography. Geophysical Research Letters 36, L09707.

Sinha, A., Stott, L.D., 1994. New atmospheric pCO_2 estimates from palesols during the late Paleocene/early Eocene global warming interval. Global and Planetary Change 9, 297–307.

Sloan, L.C., Pollard, D., 1998. Polar stratospheric clouds: A high latitude warming mechanism in an ancient greenhouse world. Geophysical Research Letters 25, 3517–3520.

Smith, R.Y., Greenwood, D.R., Basinger, J.F., 2010. Estimating paleoatmospheric pCO_2 during the Early Eocene Climatic Optimum from stomatal frequency of Ginkgo, Okanagan Highlands, British Columbia, Canada. Palaeogeography, Palaeoclimatology, Palaeoecology 293, 120–131.

Spicer, R.A., Parrish, J.T., 1990. Late Cretaceous–early Tertiary palaeoclimates of northern high latitudes: a quantitative view. Journal of the Geological Society 147, 329–341.

Stocker, T., Qin, D., Plattner, G., Tignor, M., Allen, S., Boschung, J., Nauels, A., Xia, Y., Bex, V., Midgley, P., 2013. IPCC, 2013: Summary For Policymakers in Climate Change 2013: the Physical Science basis, Contribution of Working Group I to the Fifth Assessment Report of the Intergovernmental Panel On Climate Change. Cambridge University Press, Cambridge, 1523 pp.

Stott, L.D., 1992. Higher temperatures and lower oceanic pCO_2: A climate enigma at the end of the Paleocene Epoch. Paleoceanography 7, 395–404.

Tanai, T., 1979. Late Cretaceous floras from the Kuji District, Norheastern Honshu, Japan. Journal of the Faculty of Science, Hokkaido University (Series 4), Geology and Mineralogy 19, 75–136 (in Japanese).

Tanai, T., 1990. Euphorbiaceae and Icacinaceae from the Paleogene of Hokkaido, Japan. Bulletin of the National Science Museum (Series C) 16, 91–118.

Tesfamichael, T., Jacobs, B., Tabor, N., Michel, L., Currano, E., Feseha, M., Barclay, R., Kappelman, J., Schmitz, M., 2017. Settling the issue of "decoupling" between atmospheric carbon dioxide and global temperature: $[CO_2]$atm reconstructions across the warming Paleogene–Neogene divide. Geology 45, 999–1002.

Ufnar, D.F., González, L.A., Ludvigson, G.A., Brenner, R.L., Witzke, B.J., 2004. Evidence for increased latent heat transport during the Cretaceous (Albian) greenhouse warming. Geology 32, 1049–1052.

Wang, Y., Momohara, A., Wang, L., Lebreton-Anberree, J., Zhou, Z., 2015. Evolutionary history of atmospheric CO_2 during the Late Cenozoic from fossilized *Metasequoia* needles. PLoS One 10, e0130941.

Wang, Y., Ito, A., Huang, Y.-J., Fukushima, T., Wakamatsu, N., Momohara, A., 2018a. Reconstruction of altitudinal transportation range of leaves based on stomatal evidence: An example of the Early Pleistocene *Fagus* leaf fossils from central Japan. Palaeogeography, Palaeoclimatology, Palaeoecology 505, 317–325.

Wang, Y., Momohara, A., Ito, A., Fukushima, T., Huang, Y.-J., 2018b. Warm climate under high CO_2 level in the early Pleistocene based on a leaf fossil assemblage in central Japan. Review of Palaeobotany and Palynology 258, 146–153.

Winguth, A., Shellito, C., Shields, C., Winguth, C., 2010. Climate response at the Paleocene–Eocene thermal maximum to greenhouse gas forcing — a model study with CCSM3. Journal of Climate 23, 2562–2584.

Wolfe, A.P., Reyes, A.V., Royer, D.L., Greenwood, D.R., Doria, G., Gagen, M.H., Siver, P.A., Westgate, J.A., 2017. Middle Eocene CO_2 and climate reconstructed from the sediment fill of a subarctic kimberlite maar. Geology 45, 619–622.

Yang, H., Huang, Y., Leng, Q., LePage, B.A., Williams, C.J., 2005. Biomolecular preservation of Tertiary *Metasequoia* Fossil Lagerstätten revealed by comparative pyrolysis analysis. Review of Palaeobotany and Palynology 134, 237–256.

Zachos, J., Pagani, M., Sloan, L., Thomas, E., Billups, K., 2001. Trends, rhythms, and aberrations in global climate 65 Ma to present. Science 292, 686–693.